A spectroscopic study of the G 1Π g state of 7Li2 by pulsed optical–optical double resonance

R. A. Bernheim, L. P. Gold, P. B. Kelly, T. Tipton, and D. K. Veirs

---

Articles you may be interested in

The 31Π g and 31Δ g states of 39K2 studied by optical–optical double resonance spectroscopy
J. Chem. Phys. **102**, 6966 (1995); 10.1063/1.469135

A pulsed optical–optical double resonance study of the 11Π g state of 7Li2
J. Chem. Phys. **92**, 5822 (1990); 10.1063/1.458402

A spectroscopic study of the 11Πg state of 7Li2
AIP Conf. Proc. **172**, 393 (1988); 10.1063/1.37432

A study of the E 1Σ+ g state of 7Li2 by pulsed optical–optical double resonance spectroscopy
J. Chem. Phys. **76**, 57 (1982); 10.1063/1.442705

A spectroscopic study of the E 1Σ+ g and F 1Σ+ g states of 7Li2 by pulsed optical–optical double resonance
J. Chem. Phys. **74**, 3249 (1981); 10.1063/1.441529

A spectroscopic study of the $G\ ^1\Pi_g$ state of $^7Li_2$ by pulsed optical–optical double resonance

R. A. Bernheim, L. P. Gold, P. B. Kelly, T. Tipton, and D. K. Veirs

Department of Chemistry, Davey Laboratory, The Pennsylvania State University, University Park, Pennsylvania 16802

The results of a pulsed optical–optical double resonance spectroscopic study of the $G\ ^1\Pi_g$ state of $^7Li_2$ are presented. Observations were made on the $v^* = 0$ through $v^* = 20$ levels, representing about 60% of the dissociation energy. A set of Dunham molecular constants was derived. The RKR potential was generated and Franck–Condon factors were determined for the range of observed vibrational levels. A dissociation energy was estimated from a Birge–Sponer extrapolation of the G_v values which suggests a correlation with the $(2\ ^2P) + (2\ ^2P)$ atomic lithium states at the dissociation limit.

I. INTRODUCTION

The vapors of the alkali metals were among the earliest subjects of spectroscopic study. Observations of the spectra of diatomic alkali metal molecules were made as early as 1874.[1] In the following century the alkali diatomics received considerable attention, both theoretical and experimental. Spectroscopic studies have characterized the ground and some excited states,[2] but until recently, the only excited states for these molecules that have been observed are those with *ungerade* inversion symmetry. All of the alkali diatomic molecules have $^1\Sigma_g^+$ electronic ground states, and excitation to the *gerade* states is forbidden by one-photon selection rules. Two recent studies have given evidence for excitation to a *gerade* excited state of a homonuclear alkali diatomic species. A fragment of a $^1\Sigma_g^+$ excited state in Na_2 was observed in 1976 by Woerdman, who used Doppler-free two-photon excitation.[3] In 1979 three *gerade* excited states in Na_2 were identified and partially characterized by Carlson, Kowalski, Teets, and Schawlow using a two-step polarization labeling process.[4]

Our investigations[5,6] have been concerned with the excited *gerade* states of Li_2, which is perhaps the most interesting alkali diatomic since it is the least complex stable homonuclear diatomic molecule with the exception of molecular hydrogen. Li_2 has been the subject of over 100 publications including *ab initio* and semi-empirical theoretical treatments as well as spectroscopic studies. A recent comprehensive summary of the pertinent experimental and theoretical literature has been given by Hessel and Vidal.[7]

A very complex multiphoton excitation spectrum of Li_2 is obtained in experiments conducted with a single tunable cw dye laser. A spectacular simplification is obtained through the use of pulsed optical–optical double resonance (OODR) spectroscopy with two independently tunable dye lasers.[5] In the energy region between 27 000 and 50 000 cm^{-1} above the ground state of Li_2 we have discovered and characterized a number of hitherto unobserved *gerade* excited states.[5,6]

The present work describes a careful characterization of one of these states, which we have labeled $G\ ^1\Pi_g$ and for which we have previously reported preliminary results.[5] A set of molecular constants obtained from a Dunham type analysis is given as well as a RKR potential curve and Franck–Condon factors for the transition from the $A\ ^1\Sigma_u^+$ state. The range of vibrational levels which were observed for $G\ ^1\Pi_g$ are $v^* = 0$ through $v^* = 20$. A dissociation energy was estimated from a Birge–Sponer extrapolation of the G_v values, and its relationship to the dissociation energy of the ground electronic state is discussed.

II. EXPERIMENTAL

The use of two independently tunable cw dye lasers to probe a new molecular state from different levels of a known intermediate state has been described by Gottscho, Koffend, and Field.[8] In the present experiments two independently tunable pulsed lasers were employed making possible a simplification of the observed spectra through control of the amount of relaxation permitted in the intermediate state. The experimental arrangement for the present investigation was similar to that described earlier[5] and is shown in Fig. 1. The sample cell was a cruciform heat pipe oven containing several grams of lithium (99.99% ^7Li) and was initially filled with about 30 Torr of helium at room temperature. The center of the cell was operated at approximately 800 °C while the arms remained at room temperature. Rough estimates of the partial pressures of the species present in the center of the heat pipe oven where the measurements were made are 70 Torr He, 0.1 Torr Li_2, and 2.6 Torr Li. The pump dye laser was constructed according to the design of Hänsch.[9] A Molectron DL-300 dye laser was used for the probe laser. Both pump and probe dye lasers were operated without etalon tuning elements, and both produced radiation linewidths of 0.3 cm^{-1}. Both dye lasers were pumped by vertically splitting the output beam of a Molectron UV-1000 nitrogen laser operating at 10 pulses/sec and producing 700 kW at 337.1 nm. $A\ ^1\Sigma_u^+ - X\ ^1\Sigma_g^+$ pump transitions were selected which were strong, unambiguously assigned, and not overlapped with other transitions. A fast gated integrator was used to discriminate against scattered laser radiation when detection in the visible spectral region was required. This was particularly useful when tuning the pump laser wavelength for maximum fluorescence from the chosen $A\ ^1\Sigma_u^+ - X\ ^1\Sigma_g^+$ transition. The probe laser was adjusted such that its beam overlapped that of the pump laser within the heat pipe cell. Upon scanning the probe
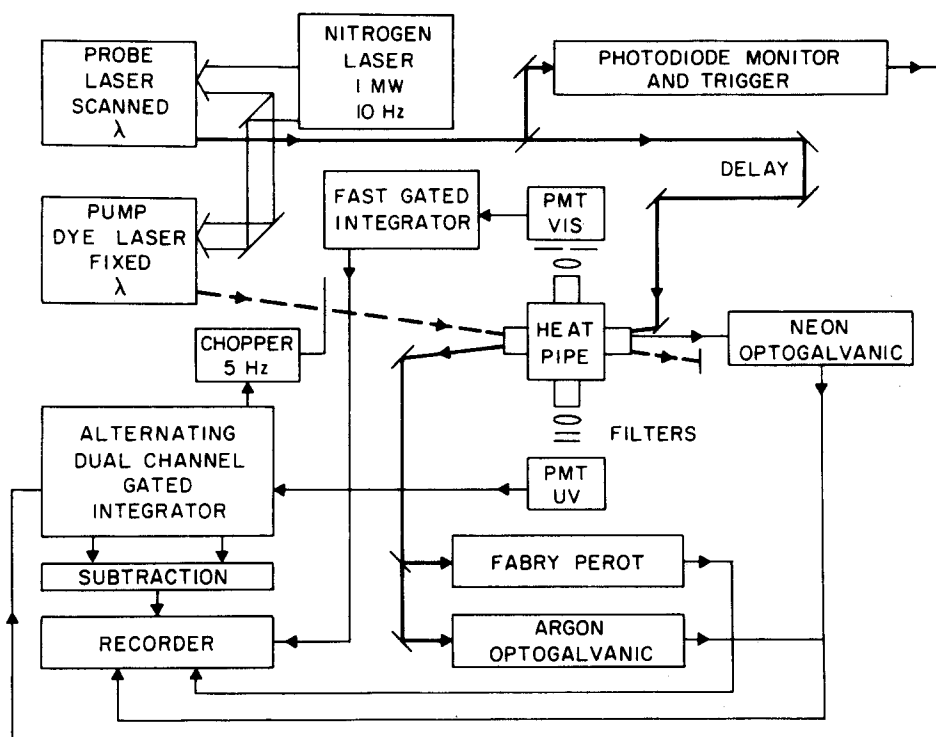
FIG. 1. Schematic diagram for the pulsed optical–optical double resonance apparatus. The neon optogalvanic cell is excited by a reflection of the probe laser beam from one of the heat pipe cell windows.

laser wavelength the vibrational bands arising from excitation to the $G\,^1\Pi_g$ state were detected by monitoring the UV emission from the heat pipe cell. The UV emission was imaged on the photocathode of a 1P28 photomultiplier tube after passing through a set of filters consisting of one Corion SB-1.25, one Schott UG-11 (1 mm), and one Corning 7-54 filter. This arrangement has a neutral density greater than 4 at wavelengths above 360 nm, passes 5% at 350 nm, and has a peak transmission of 55% at 305 nm. The UV emission shows vibrational band structure when dispersed and is, therefore, molecular in origin. Although the details of the production of UV emission are still under investigation, it is likely that one contributing mechanism involves collisional transfer of the $G\,^1\Pi_g$ lithium molecules to the neighboring $C\,^1\Pi_u$ or $D\,^1\Pi_u$ states from which single photon UV transitions are allowed to the ground state.

The powers at which the pump and probe lasers operated varied throughout the experiments depending upon which intermediate levels were chosen for excitation and upon the gain curves of the various dyes used. The pump laser was operated between 0.02 and 0.15 mJ/pulse. The lower powers were used in cases where the intermediate level is easily populated, e.g., $A\,^1\Sigma_u^+(v=1)$, which permitted the probe laser to be operated at higher power levels. In cases where the intermediate levels are more difficult to populate, which is the case for the higher vibrational levels of the $A\,^1\Sigma_u^+$ state, more pump power was needed. The probe dye laser was operated so as to deliver between 0.02 and 0.3 mJ/pulse, depending upon the requirements of the pump laser, the type of dye used, and the region of the dye gain curve utilized.

A great advantage accrues to the experiment if the probe laser pulse is delayed, resulting in collision-in-duced rotational relaxation within the $A\,^1\Sigma_u^+$ state prior to excitation to the $G\,^1\Pi_g$ state. If the probe laser pulse is not delayed, the main features of the OODR spectrum are just the $P(J)$, $Q(J)$, and $R(J)$ lines of the excitation from $A\,^1\Sigma_u^+$ to $G\,^1\Pi_g$, where J is the rotational level of the $A\,^1\Sigma_u^+$ being excited by the pump laser. If the probe laser pulse is delayed, rotational relaxation of $A\,^1\Sigma_u^+$ state Li_2 molecules occurs, and the subsequent excitation to $G\,^1\Pi_g$ consists of a band of rotational lines.

While cross sections for rotational relaxation were not determined in this study, it is instructive to consider the approximate number of collisions that do occur during the pulsed experiment. Rowe and McCaffery report that for Li_2 in helium, 0.4 collisions per lifetime occur under their experimental conditions of 730 °C and 6 Torr total pressure.[10] Since the measured $A\,^1\Sigma_u^+$ radiative lifetime is 18 nsec[11] this corresponds to a 15 Å^2 cross section for Li_2–He collisions. Under our experimental conditions a Li_2 molecule is estimated to make three collisions every 10 nsec (the pulse width of the dye laser). A small change in optical delay can therefore have a major effect upon the rotational relaxation. In the present experiments the optical delay was controlled to give an intense P–Q–R triplet originating from the pumped level to ensure a correct rotational quantum number assignment, while also providing for a large degree of rotational relaxation to ensure a large data base for the subsequent determination of molecular constants. For intense $G\,^1\Pi_g$–$A\,^1\Sigma_u^+$ bands rotational relaxation up to $\Delta J = 34$ was observed and line positions measured, while for the weakest bands only the P–Q–R triplet was measured with satisfactory precision.

Calibration of the OODR spectrum was achieved by simultaneously recording the spectra of neon and argon produced in optogalvanic cells and the fringes produced
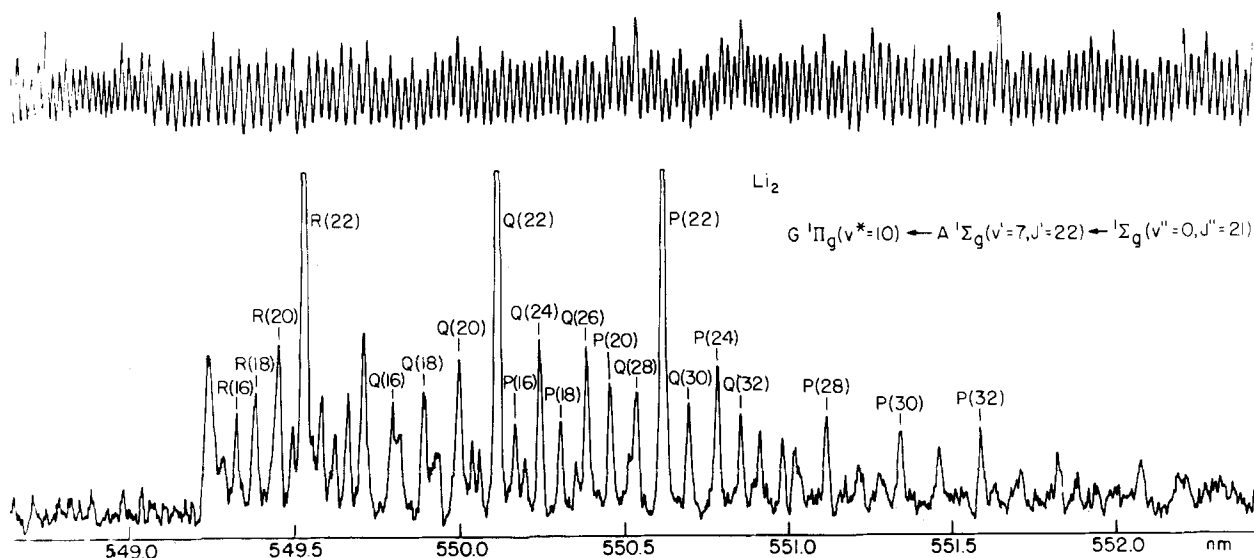
FIG. 2. Optical–optical double resonance excitation spectrum of the $G\,{}^1\Pi_g$ ($v^* = 10$) band in ${}^7\text{Li}_2$ following pumping of the $A\,{}^1\Sigma_u^+$ ($v' = 7$, $J' = 22$) level from the $X\,{}^1\Sigma_g^+$ ($v'' = 0$, $J'' = 21$) level with the pump laser tuned to 639.0402 nm. The abscissa is the probe laser wavelength in nm. The interference fringes from the Fabry–Perot etalon were separately calibrated with the optogalvanic spectra of argon and neon.

when part of the probe laser radiation was sampled by a Fabry–Perot interferometer. A typical $G\,{}^1\Pi_g$–$A\,{}^1\Sigma_u^+$ band is shown in Fig. 2. The interferometer was a Burleigh VS with 85% reflective coatings, a free spectral range of about 0.8 cm^{-1} and a finesse of 19. The OODR spectra line positions could be determined with an estimated accuracy of 0.2 cm^{-1}.

In order to distinguish the OODR spectral transitions from transitions generated by resonantly enhanced two photon excitation produced by the probe laser alone, a subtraction technique was applied. Both dye lasers were excited by the nitrogen laser at 10 Hz. The pump laser was additionally interrupted at 5 Hz. All signals that

originated from the probe laser alone were subtracted from the output of the gated integrator, and only those signals which were dependent on both lasers were retained.

III. ANALYSIS AND RESULTS

The observed data consist of approximately 600 wavelengths corresponding to transitions between known pumped levels in the $A\,{}^1\Sigma_u^+$ state and levels in the $G\,{}^1\Pi_g$ state. The constants of Kusch and Hessel[12] were used to convert each of these wavelengths to an energy referred to the bottom of the $A\,{}^1\Sigma_u^+$ state potential well. This resulted in a set of data $\nu(v^*, J^*)$ where v^* and J^* are the vibrational and rotational quantum numbers of the $G\,{}^1\Pi_g$ state level in which the corresponding transition terminated.

The vibrational assignments were made on the basis of a number of experiments as well as comparisons of the observed band intensities with calculated Franck–Condon factors. Experimentally, the vibrational levels pumped in the $A\,{}^1\Sigma_u^+$ state were $v' = 0$, 1, 2, 7, 9, and 16, and the resulting $G\,{}^1\Pi_g$ state vibrational levels which were observed excited are shown in Fig. 3. No bands
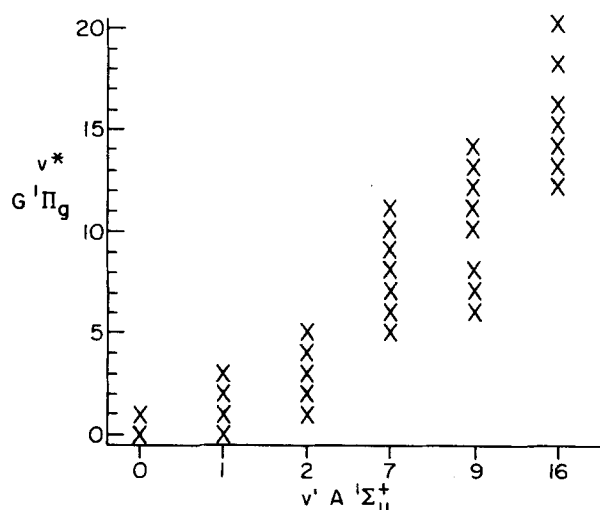
FIG. 3. Range of vibrational states v^* found in the $G\,{}^1\Pi_g$ state using different intermediate levels v', J' of the $A\,{}^1\Sigma_u^+$ intermediate state. The data for $v' = 0$ and $v' = 2$ were only used to verify the vibrational state numbering v^*, while the remaining data were used in the generation of molecular constants of the $G\,{}^1\Pi_g$ state.
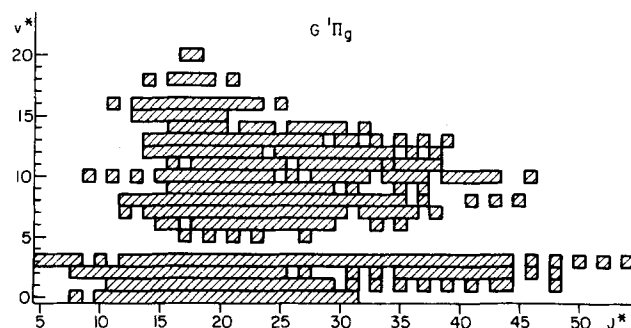

FIG. 4. Values of v^* and J^* for $G\,{}^1\Pi_g$ levels observed in these experiments.

TABLE I. Dunham coefficients that describe the $G\,{}^1\Pi_g$ state of ${}^7\text{Li}_2$ from $v^* = 0$ to $v^* = 20$. The quantities in parentheses are the exponents of 10 in the multiplying factor and all values are in cm^{-1}.

n, k	$Y_{n,k}\ (G\,{}^1\Pi_g)$	Standard error
T_e	3.1868446(+4)	4.3(−2)
1, 0	2.2926344(+2)	2.4(−2)
2, 0	−1.6246329(0)	4.9(−3)
3, 0	4.4919914(−3)	3.7(−4)
4, 0	−1.8214010(−4)	9.2(−6)
0, 1	4.6887322(−1)	9.6(−5)
0, 2	−7.6795632(−6)	8.7(−8)
0, 3	1.4537256(−10)	2.3(−11)
1, 1	−5.4766075(−3)	3.6(−6)
q	1.1514943(−3)	1.6(−5)

below that assigned to $v^* = 0$ were observed when the $v' = 0$ and $v' = 1$ levels of the $A\,{}^1\Sigma_u^+$ state were pumped.

These data were then fit by a least-squares procedure with an equation of the form

$$\nu(v, J) = \sum_{n,k} (v + \tfrac{1}{2})^n \left[J(J+1) - 1\right]^k + \delta q J(J+1) \ , \tag{1}$$

where $\delta = 0$ for the lower d levels which give rise to the Q lines ($\Delta J = 0$), and $\delta = 1$ for the upper c levels which give rise to the R and P lines ($\Delta J = \pm 1$). The factor q is a constant which measures the magnitude of the lambda doubling in the $G\,{}^1\Pi_g$ state. Preliminary analyses served to eliminate perturbed lines and transitions to other states. In the final analysis 10 constants were fitted to 521 observations.[13] The $G\,{}^1\Pi_g$ state vibrational and rotational levels used in the fit are shown in Fig. 4. The standard error of the fit was 0.14 cm^{-1}; this is consistent with the precision of the measurements. The constants so obtained are given in Table I. The value of T_e is referred to the bottom of the $X\,{}^1\Sigma_g^+$ ground state potential with the value of 1.4068307×10^4 cm^{-1} found by Kusch and Hessel for the $A\,{}^1\Sigma_u^+$ state.[12]

The observed value of $Y_{02} = -7.68 \times 10^{-6}$ cm^{-1} is within 2% of the value -7.84×10^{-6} cm^{-1} calculated from the approximate relation

$$Y_{02} = 4Y_{01}^3 / Y_{10}^2 \ , \tag{2}$$

which holds for most diatomic molecules.[14] The lambda doubling constant $q = 1.15 \times 10^{-3}$ cm^{-1}, observed for this state is about five times larger than that for the $B\,{}^1\Pi_u$ state.[7] This is consistent with the larger number of possible perturbing states near the $G\,{}^1\Pi_g$ state.

These molecular constants were used to calculate a Rydberg–Klein–Rees (RKR) potential curve with a computer program originally developed by Zare[15] which gives as output the RKR turning points for the observed vibrational levels. These are given in Table II together with the values of

$$G_v = \sum_{n=1} Y_{n0}(v + \tfrac{1}{2})^n \ , \tag{3}$$

$$B_v = \sum_{n=0} Y_{n1}(v + \tfrac{1}{2})^n \tag{4}$$

used by the RKR program and calculated from the constants in Table I.

Another program developed by Zare[15] was used to calculate Franck–Condon factors from the RKR potential curve. The results, given in Table III, are in good agreement with observation, confirming the $G\,{}^1\Pi_g$ state vibrational assignments. The program also back-calculates values of G_v and B_v from the RKR potential. The agreement between the sets of values is comparable to the agreement previously reported for the $A\,{}^1\Sigma_u^+$ state.[12]

The previously studied $A\,{}^1\Sigma_u^+$ and $B\,{}^1\Pi_u$ states correlate with the $(2\,{}^2S) + (2\,{}^2P)$ atomic lithium states in the dissociation limit.[7,12] The bound singlet states that are immediately above the $A\,{}^1\Sigma_u^+$ and $B\,{}^1\Pi_u$ states in energy correlate with the lithium atomic states as shown in Table IV. Our preliminary survey indicates that of the lowest seven singlet *gerade* states in Table IV, we have observed all but the ${}^1\Delta_g$ states. We would not expect to observe ${}^1\Delta_g$ states since the intermediate levels that were pumped all belonged to the $A\,{}^1\Sigma_u^+$ state. The $G\,{}^1\Pi_g$ state which is the subject of the present work was the lowest ${}^1\Pi_g$ observed, with two other ${}^1\Pi_g$ states being found at higher energies. For this reason we correlate the $G\,{}^1\Pi_g$ state with the $(2\,{}^2P) + (2\,{}^2P)$ lithium atomic states in the dissociation limit.

Of the remaining singlet *gerade* states, we have observed[6,16] two ${}^1\Sigma_g^+$ states which occur at energies below the $G\,{}^1\Pi_g$ state. We suggest that the lowest of these $E\,{}^1\Sigma_g^+$ correlates with the $(2\,{}^2S) + (3\,{}^2S)$ lithium atomic

TABLE II. G_v values, rotational constants B_v, and RKR potential curve for the lower d Λ-doublet levels of the $G\,{}^1\Pi_g$ state of ${}^7\text{Li}_2$ for $J = 0$.

v	G_v (cm^{-1})[a]	B_v (cm^{-1})[a]	r_{min} (Å)	r_{max} (Å)
−0.5	0	0.4688732	3.20144	
0	114.226	0.4661349	3.00891	3.41962
1	340.254	0.4606583	2.88233	3.59794
2	563.068	0.4551817	2.80164	3.73102
3	782.686	0.4497051	2.73970	3.84601
4	999.121	0.4442285	2.68867	3.95076
5	1212.384	0.4387519	2.64497	4.04886
6	1422.480	0.4332753	2.60663	4.14234
7	1629.409	0.4277987	2.57239	4.23243
8	1833.167	0.4223221	2.54144	4.32001
9	2033.747	0.4168454	2.51318	4.40570
10	2231.136	0.4113688	2.48717	4.48997
11	2425.318	0.4058922	2.46306	4.57319
12	2616.271	0.4004156	2.44060	4.65568
13	2803.969	0.3949390	2.41956	4.73770
14	2988.384	0.3894624	2.39976	4.81948
15	3169.480	0.3839858	2.38106	4.90122
16	3347.219	0.3785092	2.36332	4.98312
17	3521.558	0.3730326	2.34644	5.06536
18	3692.450	0.3675560	2.33030	5.14811
19	3859.842	0.3620794	2.31483	5.23154
20	4023.680	0.3566028	2.29994	5.31583

[a]Calculated from Eqs. (3) and (4) and the constants in Table I.

TABLE III. Franck–Condon factors ($\times 10^3$) for the $G\,^1\Pi_g\,(v^*)-A\,^1\Sigma_u^+\,(v')$ transition of $^7Li_2$ for $J=0$.

v^*/v'	0	1	2	3	4	5	6	7	8	9	10	11	12	13	14	15	16	17	18	19	20
0	893	101	6																		
1	100	699	184	16	1																
2	6	181	530	250	32	2															
3		18	243	385	299	51	3														
4		1	35	286	265	331	75	6													
5			3	56	312	170	348	101	10	1											
6				6	81	321	97	350	129	15	1										
7					10	107	315	46	339	158	22	2									
8					1	17	133	297	15	317	187	31	3								
9						1	26	158	268	1	286	214	42	4							
10							3	37	180	231	2	247	239	55	6						
11								5	50	197	190	15	205	259	70	8	1				
12									8	66	209	147	35	161	275	87	12	1			
13									1	12	83	214	106	59	118	284	106	16	1		
14										1	18	100	212	69	85	80	287	126	22	2	2
15										2	26	118	201	39	108	48	283	146	28		2
16											4	35	134	185	17	126	23	272	166		36
17												6	46	147	162	4	137	8	256		185
18													1	10	59	158	138		142	1	239
19														1	14	73	167	116		2	143
20															2	19	86	174	104	6	144

states, while the other $F\,^1\Sigma_g^+$ correlates with $(2\,^2P)+(2\,^2P)$ in common with the $G\,^1\Pi_g$ state.

Estimation of the dissociation energy D_e for the $G\,^1\Pi_g$ state is complicated by the relatively large uncertainties in the dissociation energies for the ground state and the $A\,^1\Sigma_u^+$ state; these have been reviewed by Konowalow and Olson.[17] While the value of D_e that can be obtained for the $G\,^1\Pi_g$ state does not have sufficient reliability to remove the uncertainties in D_e for the $X\,^1\Sigma_g^+$ and $A\,^1\Sigma_u^+$ states, it is consistent with the correlation of $G\,^1\Pi_g$ with the $(2\,^2P)+(2\,^2P)$ atomic lithium states made above. The "most likely" value of $D_e = 8450$ cm^{-1} of Konowalow and Olsen for the $X\,^1\Sigma_g^+$ state has been estimated to be good to ± 100 cm^{-1}. Combined with the value of T_e for the $G\,^1\Pi_g$ found in this work and the atomic excitation values in Table IV, a value of $D_e = 6390$ cm^{-1} is found if $G\,^1\Pi_g$ correlates with $(2\,^2P)+(2\,^2P)$, while a value of $D_e = 7507$ cm^{-1} results if $G\,^1\Pi_g$ correlates with $(2\,^2S)+(3\,^2P)$. A nonlinear extrapolation of the G_v values calculated from the constants in Table I gives $D_e = 6830$ cm^{-1}. However, the Dunham coefficients in Table I accurately describe

only that part of the potential which is represented by the observed data, and extrapolations beyond this range are often not very reliable.[12,18] While the estimated value of D_e for $G\,^1\Pi_g$ cannot by itself distinguish between the two choices of pairs of atomic lithium states which correlate with $G\,^1\Pi_g$, we assign the $(2\,^2P)+(2\,^2P)$ pair on the basis that no other $^1\Pi_g$ state was observed in the 5000 cm^{-1} range below $G\,^1\Pi_g$. The $G\,^1\Pi_g$ state measurements extend to $v^* = 20$ where the energy is 4024 cm^{-1} or about 60% of the estimated dissociation energy.

The possibility exists for a detailed study of the upper portion of the $G\,^1\Pi_g$ state from which a reliable value of the dissociation energy might be obtained. This continues to be of some importance since it would resolve the small uncertainty that currently exists for the dissociation energy of the $X\,^1\Sigma_g^+$ state.[7] The possibility also exists for an accurate theoretical extrapolation of the upper portion of the potential curve as has been done for the $X\,^1\Sigma_g^+$ and $A\,^1\Sigma_u^+$ states.[17]

In conclusion, this investigation has for the first time reported the observation and analysis of a *gerade* excited electronic state of $^7Li_2$. It appears that the lower 60% of the state is now known with reasonable accuracy and includes the first 20 vibrational levels.

ACKNOWLEDGMENT

TABLE IV. Correlation of pairs of lithium atomic states with Li_2 molecular states.

Atomic states	Excitation energy[a] (cm^{-1})	Singlets		Triplets	
		g	u	g	u
$2\,^2S+3\,^2S$	27 206	$^1\Sigma_g^+$	$^1\Sigma_u^+$	$^3\Sigma_g^+$	$^3\Sigma_u^+$
$2\,^2P+2\,^2P$	29 808	$^1\Sigma_g^+$, $^1\Sigma_g^+$ $^1\Pi_g$, $^1\Delta_g$	$^1\Sigma_u^-$, $^1\Pi_u$	$^3\Sigma_g^-$, $^3\Pi_g$	$^3\Sigma_u^+$, $^3\Sigma_u^+$ $^3\Pi_u$, $^3\Delta_u$
$2\,^2S+3\,^2P$	30 925	$^1\Sigma_g^+$, $^1\Pi_g$	$^1\Sigma_u^+$, $^1\Pi_u$	$^3\Sigma_g^+$, $^3\Pi_g$	$^3\Sigma_u^+$, $^3\Pi_u$
$2\,^2S+3\,^2D$	31 283	$^1\Sigma_g^+$, $^1\Pi_g$ $^1\Delta_g$	$^1\Sigma_u^+$, $^1\Pi_u$ $^1\Delta_u$	$^3\Sigma_g^+$, $^3\Pi_g$ $^3\Delta_g$	$^3\Sigma_u^+$, $^3\Pi_u$ $^3\Delta_u$

[a]Measured with respect to the $2\,^2S+2\,^2S$ pair of atomic Li states.

[1] H. E. Roscoe and A. Schuster, Proc. R. Soc. London 22, 362 (1874).
[2] K. P. Huber and G. Herzberg, *Molecular Spectra and Molecular Structure*, Vol. IV (Van Nostrand Reinhold, New York, 1979).
[3] J. P. Woerdman, Chem. Phys. Lett. 43, 279 (1976).
[4] N. W. Carlson, F. V. Kowalski, R. E. Teets, and A. L.

Schawlow, Opt. Commun. **29**, 302 (1979).

[5] R. A. Bernheim, L. P. Gold, P. B. Kelly, C. Kittrell, and D. K. Veirs, Phys. Rev. Lett. **43**, 123 (1979).

[6] R. A. Bernheim, L. P. Gold, P. B. Kelly, C. Kittrell, and D. K. Veirs, Chem. Phys. Lett. **70**, 104 (1980).

[7] M. M. Hessel and C. R. Vidal, J. Chem. Phys. **70**, 4439 (1979).

[8] R. A. Gottscho, J. B. Koffend, and R. W. Field, J. Chem. Phys. **68**, 4110 (1978).

[9] T. W. Hänsch, Appl. Opt. **11**, 895 (1972).

[10] M. D. Rowe and A. J. McCaffery, Chem. Phys. **34**, 81 (1978).

[11] P. H. Wine and L. A. Melton, Chem. Phys. Lett. **45**, 509 (1977).

[12] P. Kusch and M. M. Hessel, J. Chem. Phys. **67**, 586 (1977).

[13] See AIP document No. PAPS JCPSA-74-2749-14 for 14 pages containing observed spectral transitions, assignments, differences between observed and calculated spectral energies, and the variance–covariance and correlation matrix for the molecular constants. Order by PAPS number and journal reference from American Institute of Physics, Physics Auxiliary Publication Service, 335 East 45th Street, New York, N. Y. 10017. The price is $1.40 for microfiche or $5.00 for photocopies. Airmail additional. Make check payable to the American Institute of Physics.

[14] G. Herzberg, *Molecular Spectra and Molecular Structure*, Vol. I, 2nd edition (Van Nostrand, Princeton, N. J., 1950).

[15] W. Demtröder, M. McClintock, and R. N. Zare, J. Chem. Phys. **51**, 5495 (1969).

[16] R. A. Bernheim, L. P. Gold, P. B. Kelly, C. A. Tomczyk, and D. K. Veirs (unpublished).

[17] D. D. Konowalow and M. L. Olson, J. Chem. Phys. **71**, 450 (1979).

[18] D. L. Albritton, A. L. Schmeltekopf, and R. N. Zare, in *Molecular Spectroscopy: Modern Research*, Vol. II, edited by K. N. Rao (Academic, New York, 1976), p. 1.